New palladium(II) complexes with pyrazole ligands

Part II. Synthesis, spectral and thermal studies, and antitumor evaluation

Carolina V. Barra · Fillipe V. Rocha · Adelino V. G. Netto ·
Regina C. G. Frem · Antonio E. Mauro · Iracilda Z. Carlos ·
Sandra R. Ananias · Marcela B. Quilles

Abstract This study describes the synthesis, IR, ^{1}H, and ^{13}C{^{1}H} NMR spectroscopic as well the thermal characterization of the new palladium(II) pyrazolyl complexes [PdCl$_2$(HmPz)$_2$] **1**, [PdBr$_2$(HmPz)$_2$] **2**, [PdI$_2$(HmPz)$_2$] **3**, [Pd(SCN)$_2$(HmPz)$_2$] **4** {HmPz = 4-methylpyrazole}. The residues of the thermal decomposition were identified as Pd^0 by X-ray powder diffraction. From the initial decomposition temperatures, the thermal stability of the complexes can be ordered in the sequence: **1 > 2 > 4 ≈ 3**. The cytotoxic activities of the complexes and the ligand were investigated against two murine cancer cell lines: mammary adenocarcinoma (LM3) and lung adenocarcinoma (LP07) and compared to cisplatin under the same experimental conditions.

Introduction

A great deal of interest has been devoted to metal-based compounds bearing pyrazolyl-type ligands due to their interesting structures and potential uses [1–3]. In particular,

C. V. Barra · F. V. Rocha · A. V. G. Netto (✉) ·
R. C. G. Frem · A. E. Mauro
Departamento de Química Geral e Inorgânica, Instituto de Química de Araraquara, UNESP-Univ Estadual Paulista, 355, Araraquara, SP 14801-970, Brazil
e-mail: adelino@iq.unesp.br

I. Z. Carlos · S. R. Ananias · M. B. Quilles
Departamento de Análises Clínicas, Faculdade de Ciências Farmacêuticas de Araraquara, UNESP-Univ Estadual Paulista, 502, Araraquara, SP 14801-902, Brazil

the antitumor activities of pyrazolyl complexes have been widely investigated since many of them have displayed cytotoxicity comparable or superior than the standard drugs. For instance, compounds of the type [{AuCl$_2$(L)}$_2$] (L = pyrazole, 3-methylpyrazole) were more cytotoxic than cisplatin toward the MOLT-4 and C2C12 tumor cell lines [4]. Rocha et al. [5] have reported that the cytotoxic activity of the [PdI$_2$(tdmPz)] compound (tdmPz = 1-thiocarbamoyl-3,5-dimethylpyrazole) towards mammary adenocarcinoma murine tumor cell line (LM3) is comparable to the value found for cisplatin. The in vitro antitumoral assays performed with Pd(II) and Pt(II) complexes [ML$_2$] (HL = a substituted 2,5-dihydro-5-oxo-1H-pyrazolone-1-carbothioamide) showed significant cytostatic activity, with the most active derivative (a palladium complex) being about 16 times more active than cisplatin against the cisplatinum-resistant cell line A2780cisR [6].

Thermal studies on this class of complexes have also attracted considerable attention since pyrazolyl metal-based compounds can display desirable properties of precursors in chemical vapor deposition (CVD) film growth processes such as high thermal stability, and suitable volatility below the decomposition temperature, and so on [7, 8].

As a part of our ongoing research interest in thermal behavior [9–13], biological activity [14–17], and structural aspects [18–23] of metal-based complexes, we describe herein the synthesis, spectroscopic characterization, and thermal studies on the compounds [PdCl$_2$(HmPz)$_2$] **1**, [PdBr$_2$(HmPz)$_2$] **2**, [PdI$_2$(HmPz)$_2$] **3**, [Pd(SCN)$_2$(HmPz)$_2$] **4** {HmPz = 4-methylpyrazole}. The cytotoxic activities of the complexes and the ligand were investigated against two murine cancer cell lines: mammary adenocarcinoma (LM3) and lung adenocarcinoma (LP07) and compared to cisplatin under the same experimental conditions.

Experimental

General comments

4-Methylpyrazole was purchased from Acros Organics. The materials employed in the syntheses were all commercially available and were used without purification. All the solvents were dried and stored over molecular sieves before use. The starting complex [PdCl$_2$(MeCN)$_2$] was prepared as described in [17].

Synthesis of the complexes

Compound [PdCl$_2$(HmPz)$_2$] **1** was prepared from the addition of 32 mg (0.39 mmol) of 4-methylpyrazole, in 2 mL of CH$_3$OH, to a deep orange solution containing 50 mg (0.19 mmol) of [PdCl$_2$(MeCN)$_2$], in 10 mL of CH$_3$OH. After stirring for 1 h, the solvent of the light orange solution was slowly evaporated, resulting an orange solid. The obtained yield was 51%. Compounds **2–4** were synthesized as follows: 3 mL of a methanolic solution containing the 4-methylpyrazole (32 mg, 0.39 mmol) was added dropwise to a deep orange solution of [PdCl$_2$(MeCN)$_2$] (50 mg, 0.19 mmol) in 10 mL of CH$_3$OH. After stirring for 1 h, 0.27 mmol of the appropriate potassium salt (KX) was added (X = Br, I, SCN) dissolved in 1 mL of water. The mixtures were stirred magnetically for 1 h. After the slow evaporation of solvents, crystalline solids have been obtained. Yields: 40–60%.

Instrumentation

Elemental analyses of carbon, nitrogen, and hydrogen were performed on a microanalyzer elemental analyzer CHN, model 2400 Perkin-Elmer. Infrared spectra were recorded in KBr pellets on a Nicolet model SX-FT-Impact 400 spectrophotometer in the 4000–400 cm^{-1} spectral range at a resolution of 4 cm^{-1}. ^{1}H- and ^{13}C{^{1}H} NMR spectra were recorded in dmso-d_6 solutions at room temperature on a Varian INOVA 500 spectrometer. Melting points were determined on a MAPFQ apparatus. Thermal analyses (TG) and differential thermal analyses (DTA) were carried out using a TA Instruments model SDQ 600, under flow of dry synthetic air (50 mL min^{-1}), temperature up to 900 °C, and at heating rate of 20 °C min^{-1} in α-alumina sample holders. The reference substance was pure α-alumina in DTA measurements. X-ray powder diffraction patterns were measured on a Siemens D-5000 X-ray diffractometer using CuKα radiation ($k = 1.541$ Å) and setting of 34 kV and 20 mA. The peaks were identified using ICDD bases [24].

MTT assay

For the cytotoxicity evaluation, 200.0 μL samples of LM3, and LP07 cells (5×10^4 cell mL^{-1}, adjusted in MEM) [5], were added to each well of a 96-well tissue culture plate (Corning) and then preincubated in the absence of compounds for 24 h to allow adaptation of cells before the addition of the test agents. Then, supernatants were removed, and 200.0 μL of the compounds in concentrations ranging from 2 to 140 μM or 200.0 μL of MEM-complete as cell control of viability was added to each well. The effects of the compounds under the cells were determined 24 h after culture incubation. Then, supernatants were removed, and 100.0 μL of solution of [3-(4,5-dimethylthiazol-2-yl)-2,5-diphenyltetrazolium bromide] (MTT) was added in each well containing the samples [25]. MTT assay was performed, and the plates were incubated for 3 h. Then, absorbances were measured, and the cytotoxic midpoint value, the concentration of chemical agent needed to reduce the spectrophotometric absorbance to 50%, was determined by linear regression analysis with 95% of confidence limits. The IC$_{50}$ was defined as the medium of two independent experiments through the equation of graphic line obtained (Microcal Origin 5.0$^{™}$). Each compound in a given concentration was tested in triplicates in each experiment.

Results and discussion

The elemental analyses and thermogravimetric data, together with IR, ^{1}H, and ^{13}C{^{1}H} NMR spectroscopic results confirmed lead us to suggest the formulae illustrated in Fig. 1. The analytical data and melting points are shown in Table 1.

Infrared spectra

The most significant bands of the ligand and the complexes with their assignments are presented in Table 2. IR experiments revealed the neutral monodentate coordination
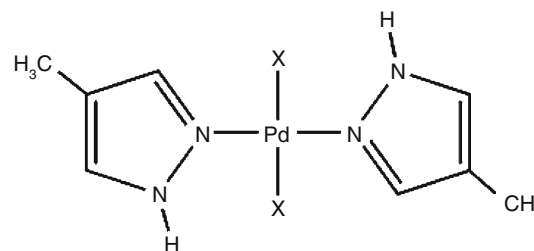

Fig. 1 Proposed structure of the compounds [PdX$_2$(HmPz)$_2$] (X = Cl **1**, Br **2**, I **3**, SCN **4**)

Table 1 Results of chemical analyses and melting points of the compounds **1–4**

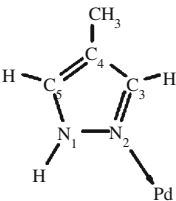| Complex	m.p./°C	Found/calcd./%		
		C	H	N
1	248 (dec)	28.09/28.13	3.51/3.54	16.29/16.40
2	206 (dec)	22.01/22.32	2.95/2.81	13.58/13.02
3	200 (dec)	18.16/18.32	2.20/2.31	10.97/10.68
4	160 (dec)	30.95/31.05	3.08/3.13	21.86/21.73

of 4-methylpyrazole by the appearance of the typical νNH bands over the spectral range of 3300–3130 cm^{-1} and by the shift of the absorption band attributed to the ring breathing mode to lower frequency (1571 cm^{-1}) when compared with that one of the free ligand (1577 cm^{-1}) [26]. The number of bands attributed to γCH vibrational modes can be also used as diagnosis for pyrazole coordination fashion since two γCH bands are expected for neutral monodentate 4-substituted pyrazoles [27]. The appearance of the two γCH bands at ca. 861 and 827 cm^{-1} for **1–4** and $\sim$857 and 662 cm^{-1} for **5–8** strongly supports the monodentate character of pyrazole instead of a single γCH absorption for exo-bidentate pyrazole complexes. The terminal *S*-bonded coordination of thiocyanate in **4** was evidenced by the appearance of an intense and sharp band at 2115 cm^{-1} (ν_{as}SCN) [28].

^{1}H and ^{13}C{^{1}H} NMR spectra

Table 3 lists the ^{1}H and ^{13}C{^{1}H} NMR results obtained to **1–4**.

^{1}H and ^{13}C{^{1}H} NMR spectra unambiguously indicated the formation of the mononuclear Pd(II) compounds and showed good agreement with our earlier reports [29]. The neutral monodentate mode of 4-methylpyrazole is indicated in the ^{1}H-NMR spectra of **1–4** by the non-equivalence of the protons at position three and five and by the existence of the NH signal at ca. 13–14 ppm. Besides the typical signals of the pyrazolyl ring, the ^{13}C{^{1}H} NMR spectrum of **4** also exhibited a resonance at $\sim$117 ppm assigned to the carbon atom from the *S*-thiocyanato group [30].

Thermogravimetric analysis

The TG and DTA curves for the compounds [PdCl$_2$(HmPz)$_2$] **1**, [PdBr$_2$(HmPz)$_2$] **2**, [PdI$_2$(HmPz)$_2$] **3**, [Pd(SCN)$_2$(HmPz)$_2$] **4** are shown in Fig. 2. Table 4 lists the initial and final temperatures (°C), partial mass losses (%), and DTA peaks of the thermal studies on compounds **1–4** together with the assignments of each decomposition stage based on mass calculation. Therefore, the groups indicated at the right column of the Table 4 do not correspond necessarily to the gaseous final products of decomposition.

Table 2 Selected infrared frequencies (cm^{-1}) for HmPz and compounds **1–4**

	νNH	νCH	νCH$_3$	ν_{ring}	δCH$_3$	δCH	νNN	γCH	γ_{ring}
HmPz	3,500–2,500 *br*	a		1,580 w	1,460 m	1,225 m	951 s	858 m, 804 m	563 w
1	3,325 s	3,134 m	2,925 w	1,571 w	1,483 m	1,128 s	1,076 m	862 m, 829 m	576 m
2	3,321 s	3,132 m	2,925 w	1,571 w	1,481 m	1,128 s	1,074 m	860 m, 829 m	578 m
3	3,269 s	3,111 m	2,925 w	1,571 w	1,483 m	1,137 s	1,078 m	860 m, 821 m	574 m
4	3,134 s	3,074 m	2,977 w	1,577 w	1,475 m	1,145 m	1,080 m	860 m, 831 m	607 m

ν = stretching, δ = in-plane bending, γ = out-of-plane bending, s = strong, m = medium, w = weak, a Uncovered

Table 3 ^{1}H and ^{13}C{^{1}H} NMR data (ppm) for compounds **1–4** at 298 K, in dmso-d_6

Numbering scheme		^{1}H-NMR data^a				^{13}C{^{1}H}-NMR data				
		NH	H$_3$	H$_5$	CH$_3$	C$_3$	C$_4$	C$_5$	CH$_3$	SCN
	1	12.90	7.65	7.60	2.02	141.09	115.79	131.06	8.42	–
	2	13.18	7.64	7.58	2.01	141.06	115.96	131.16	8.38	–
	3	13.39	7.63	7.47	1.98	143.73	116.32	131.22	8.42	–
	4	13.71	7.77	7.63	2.05	141.04	114.96	132.89	8.54	117.42

^{a} All signals were found as singlets

Fig. 2 TG and DTA curves of the complexes [PdX$_2$(HmPz)$_2$] (X = Cl **1**, Br **2**, I **3**, SCN **4**)

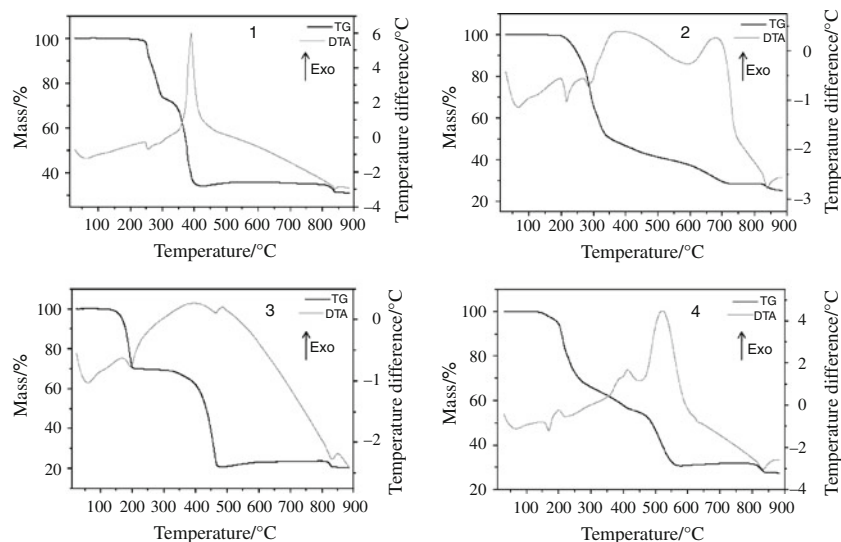**Table 4** Thermal analysis data for compounds [PdX$_2$(HmPz)$_2$] (X = Cl **1**, Br **2**, I **3**, SCN **4**)

Complex	Step	$\Delta T/°C$	$\Delta m/\%$		DTA peaks/°C		Assignment
			Obt.	Calc.	Endo	Exo	
1	1	231–305	−28.4	−28.1	256	–	−2Cl$^-$, −2CH$_3$, 0.15O$_2$
	2	305–422	−37.3	−37.9	–	390	Organic compounds, 0.15O$_2$
	3	422–792	1.7	1.9	–	–	0.2O$_2$
	4	792–865	−4.7	−4.7	838	–	−0.5O$_2$
	Residue		31.4	31.2			
2	1	187–718	−71.4	−71.9	216	–	−2Br$^-$, −2HmPz, 0.45O$_2$
	2	718–818	0.1	0.4	–	–	0.05O$_2$
	3	818–878	−3.3	−3.7	837	–	−0.5O$_2$
	Residue		25.2	24.7			
3	1	131–206	−30.1	−31.3	196	–	−2HmPz
	2	206–473	−49.2	−48.1	–	–	−2I$^-$, 0.05O$_2$
	3	473–811	2.9	2.7	–	–	0.45O$_2$
	4	811–859	−3.3	−3.0	832	–	−0.5O$_2$
	Residue		20.4	20.3			
4	1	134–574	−69.4	−70.0	166	416, 522	−2SCN$^-$, −2HmPz, 0.3O$_2$
	2	574–775	1.2	1.6	–	–	0.2O$_2$
	3	775–865	−4.3	−4.1	832	–	−0.5O$_2$
	Residue		27.6	27.5			

The TG curves of these compounds showed a similar thermal degradation pattern in which the ligands are initially released in one or two stages, together with uptake of O$_2$, leading to a mixture of Pd (ASTM 05-0681) and PdO (ASTM 06-0515). After this stage, the TG curves of the compounds exhibited a slight mass increase up to ca. 800 °C due to the oxidation of the remaining Pd^0 to PdO. Finally, the decomposition of PdO to Pd^0 is completed at ∼865 °C.

The TG curve showed that the thermal degradation pattern of **1** consists of the gradual elimination of the 4-methylpyrazole ligand during the initial decomposition steps between 231 and 422 °C. In this range, a weight loss of 65.6% is caused by the elimination of the pyrazolyl ligands and the chlorides with uptake of O$_2$ (calculated. 66.0%). It affords a mixture of Pd^0 + PdO. In the third step, a slight mass gain of 1.7% is ascribed to the oxidation of the remaining Pd^0 to PdO (calculated. 1.9%). The degradation of PdO to Pd^0 (Calcd. 31.2%, Found 31.4%) is observed between 792 and 865 °C.

In the range 187–718 °C, compound **2** loses the organic (HmPz) and inorganic (Br) ligands ($\Delta m = -71.4\%$), with

uptake of O_2, yielding a mixture of Pd and PdO (calculated 71.9%). The TG curve also exhibits a progressive mass gain up to 818 °C due to the partial oxidation of the Pd to PdO. The last mass loss ($\Delta m = -3.3\%$) is in agreement with calculated ($\Delta m = -3.7\%$) for the decomposition of PdO to metallic palladium.

With regard to the thermal behavior of **3**, the first stage (131–206 °C) is assigned, by mass calculation, to the elimination of the pyrazolyl ligands ($\Delta m_{calcd.}$ 31.3%, Δm_{found} 30.1%) and the second stage (206–473 °C) to the loss of two iodide with uptake of O_2 leading to a mixture of $Pd^0 + PdO$ ($\Delta m_{calcd.}$ 48.1%, Δm_{found} 49.2%). The formation of additional PdO is noticed by a progressive mass gain of 2.9% observed at 473–811 °C ($\Delta m_{calcd.}$ 2.7%). The decomposition of PdO to Pd is observed in the last step between 811 and 859 °C.

Compound **4** is thermally stable up to 134 °C. Afterward, a mass change of 69.4% is caused by the elimination of the ligands with uptake of O_2 (calculated 70.0%) affording a mixture PdO + Pd. In the range 574–775 °C, additional PdO is formed, which can be noticed by the slight increase of mass. The PdO further decomposed into Pd in the last mass loss (Calcd. 27.5%, Found 27.6%).

The DTA curves of **1–4** show a series of signals associated to endothermic and exothermic decomposition processes, specially an endothermic peak corresponding to thermal decomposition of PdO to Pd^0 in the range of 832–838 °C.

Taking into account the initial decomposition temperatures, the thermal stability of the complexes varies in the sequence $[PdCl_2(HmPz)_2]$ **1** > $[PdBr_2(HmPz)_2]$ **2** > $[Pd(SCN)_2(HmPz)_2]$ **4** ≈ $[PdI_2(HmPz)_2]$ **3**. These thermoanalytical results clearly show that the thermal stability varies according to the anionic groups.

Some interesting trends can be noticed from the comparison of TG data of the complexes **1** and **4** with their analogous $[PdX_2L_2]$ {L = pyrazole (HPz); 3,5-dimethyl-pyrazole (HdmPz) [31], 3,5-dimethyl-4-iodopyrazole (HdmIPz) [32]; X = Cl, SCN}. The thermal stability of the compounds $[PdCl_2L_2]$ varies in the sequence of HdmIPz > HdmPz ≈ HmPz > HPz, indicating that the substituents on the pyrazolyl ring play an important role in their thermal stability. Complexes of general type $[Pd(SCN)_2L_2]$ display the following thermal stability HdmPz > HdmIPz ≈ HmPz ≈ HPz probably due to packing effects. This fact is supported by the crystal structure of $[Pd(SCN)_2(HdmPz)_2]$ [33] in which the monomers are involved in intermolecular hydrogen bonds whereas such interactions are absent in the crystal packing of $[Pd(SCN)_2(HPz)_2]$ [28]. The thermal stability also varies according to the anionic ligand, following the sequence Cl > SCN.

In vitro antitumor assays

The cytotoxic activities of the complexes and the ligand were investigated against two murine cancer cell lines: mammary adenocarcinoma (LM3) and lung adenocarcinoma (LP07) and compared to cisplatin under the same experimental conditions. Cells were exposed to a range of drug concentrations (140–20 μM) for 24 h, and cell viability was analyzed by MTT assay. The results reveal that no significant cytotoxic activity was observed even at the highest concentration tested (140 μM). Cisplatin was able to induce 50% of cell death (IC_{50}) at 30.3 μM (LM3) and 4.34 μM (LP07).

Conclusions

This study describes the synthesis, spectroscopic characterization, thermal studies, and in vitro antitumor evaluation of the new palladium(II) pyrazolyl complexes $[PdCl_2(HmPz)_2]$ **1**, $[PdBr_2(HmPz)_2]$ **2**, $[PdI_2(HmPz)_2]$ **3**, $[Pd(SCN)_2(HmPz)_2]$ **4**. TG curves showed that the thermal degradation pattern of **1–4** consists of the elimination of the ligands, the oxidation of the remaining Pd^0 to PdO, and the decomposition of PdO to Pd^0. The IR, ^1H, and $^{13}C\{^1H\}$ NMR experiments indicated the neutral monodentate coordination of 4-methylpyrazole. This series of palladium(II) complexes does not display cytotoxicity on the tested tumor murine cell lines.

References

1. Halcrow MA. Pyrazoles and pyrazolides—flexible synthons in self-assembly. Dalton Trans. 2009;12:2045–256.
2. Netto AVG, Frem RCG, Mauro AE. A química supramolecular de complexos pirazólicos. Quím Nova. 2008;31:1208–17.
3. Pérez J, Riera L. Pyrazole complexes and supramolecular chemistry. Eur J Inorg Chem. 2009;2009:4913–25.
4. Fan D, Yang C, Ranford JD, Vittal JJ. Chemical and biological studies of gold(III) complexes with uninegative bidentate *N*–*N* ligands. Dalton Trans. 2003;(24):4749–53.
5. Rocha FV, Barra CV, Netto AVG, Mauro AE, Carlos IZ, Frem RCG, Ananias SR, Quilles MB, Stevanato A, da Rocha MC. 3,5-Dimethyl-1-thiocarbamoylpyrazole and its Pd(II) complexes: synthesis, spectral studies and antitumor activity. Eur J Med Chem. 2010;45:1698–702.
6. Casas JS, Castellano EE, Ellena J, García-Tasende MS, Pérez-Parallé ML, Sánchez A, Sanchéz-González A, Sordo J, Touceda A. New Pd(II) and Pt(II) complexes with *N*,*S*-chelated pyrazolonate ligands: molecular and supramolecular structure and preliminary study of their in vitro antitumoral activity. J Inorg Biochem. 2008;102:33–45.
7. El-Kaderi HM, Heeg MJ, Winter CH. Synthesis, structure, and properties of monomeric strontium and barium complexes

containing terminal η2–3,5-di-tert-butylpyrazolato ligands. Polyhedron. 2005;24:645–53.

8. Singhal A, Mishra R, Kulshreshtha SK, Bernhardt PV, Tiekink ERT. Dimeric allylpalladium(II) complexes with pyrazolate bridges: synthesis, characterization, structure and thermal behavior. J Organomet Chem. 2006;691:1402–10.

9. Netto AVG, Takahashi PM, Frem RCG, Mauro AE, Zorel HE Jr. Thermal decomposition of palladium(II) pyrazolyl complexes. Part I. J Anal Appl Pyrolysis. 2004;72:183–9.

10. Fernandes RL, Takahashi PM, Frem RCG, Netto AVG, Mauro AE, Matos JR. Synthesis, spectral, and thermal studies on dicarboxylate-bridged palladium(II) coordination polymers. Part I. J Therm Anal Calorim. 2009;97:123–6.

11. Fernandes RL, Takahashi PM, Frem RCG, Netto AVG, Mauro AE, Matos JR. Synthesis, spectral and thermal studies on dicarboxylate-bridged palladium(II) coordination polymers. Part II. J Therm Anal Calorim. 2009;97:153–6.

12. Lucca Neto VA, Mauro AE, Netto AVG, Moro AC, Nogueira VM. Mono and dinuclear Pd(II) complexes with pyrazole and imidazole-type ligands. Synthesis, characterization, and thermal behaviour. J Therm Anal Calorim. 2009;97:57–60.

13. de Almeida ET, Santana AM, Netto AVG, Torres C, Mauro AE. Thermal study of cyclopalladated complexes of the type [Pd2(dmba)2X2(bpe)] (X = NO_3^-, Cl^-, N_3^-, NCO^-, NCS^-; bpe = trans-1,2-bis(4-pyridyl)ethylene). J Therm Anal Calorim. 2005;82:361–4.

14. Moro AC, Mauro AE, Netto AVG, Ananias SR, Quilles MB, Carlos IZ, Pavan FR, Leite CQF, Hörner M. Antitumor and antimycobacterial activities of cyclopalladated complexes: X-ray structure of [Pd(C2, N-dmba)(Br)(tu)] (dmba = N,N-dimethylbenzylamine, tu = thiourea). Eur J Med Chem. 2009;44:4611–5.

15. de Almeida ET, Mauro AE, Santana AM, Netto AVG. Emprego de compostos organometálicos mononucleares de paládio(II) na ativação de macrófagos peritoneais de camundongos. Quím Nova. 2005;28:405–8.

16. de Souza RA, Stevanato A, Treu-Filho O, Netto AVG, Mauro AE, Castellano EE, Carlos IZ, Pavan FR, Leite CQF. Antimycobacterial and antitumor activities of palladium(II) complexes containing isonicotinamide (isn): X-ray structure of trans-[Pd(N_3)$_2$(isn)$_2$]. Eur J Med Chem. 2010;45:4863–8.

17. Bego AM, Frem RCG, Netto AVG, Mauro AE, Ananias SR, Carlos IZ, da Rocha MC. Immunomodulatory effects of palladium(II) complexes of 1,2,4-triazole on murine peritoneal macrophages. J Brazil Chem Soc. 2009;20:437–44.

18. Santana AM, Mauro AE, de Almeida ET, Netto AVG, Klein SI, Santos RHA, Zóia JR. 1,3-Dipolar cycloaddition of CS2 to the coordinated azide in the cyclopalladated [Pd(bzan)(μ-N3)]2. Crystal and molecular structure of di(μ-N, S-1,2,3,4-thiotriazole-5-thiolate)bis[(benzylideneaniline-C2, N) palladium(II)]. J Coord Chem. 2001;53:163–72.

19. Moro AC, Watanabe FW, Ananias SR, Mauro AE, Netto AVG, Lima APR, et al. Supramolecular assemblies of cis-palladium complexes dominated by C–H···Cl interactions. Inorg Chem Commun. 2006;9:493–6.

20. Mauro AE, Caires ACF, Santos RHA, Gambardella MTP. Cycloaddition reaction of the azido-bridged cyclometallated complex [Pd(dmba)N3]2 with CS2. Crystal and molecular structure of di(μ, N, S-l,2,3,4-thiatriazole-5-thiolate)bis[(N,N-dimethylbenzyl-amine-C^2,N)palladium(II)]. J Coord Chem. 1999; 48:521–8.

21. Tomita K, Caires ACF, Neto VAD, Mauro AE. Structure of a cyclopalladated complex, [PdCl($C_{37}H_{32}N$)]. Acta Crystallogr C. 1994;50:1872–3.

22. Zukerman-Schpector J, Castellano EE, De Simone CA, Oliva G, Mauro AE. Structure of di-μ-cyanato-bis[cyanato(N,N-diethylethylenediamine)copper(II)], [Cu(NCO)2(dieten)]2. Acta Crystallogr C. 1991;47:957–9.

23. Legendre AO, Mauro AE, Ferreira JG, Ananias SR, Santos RHA, Netto AVG. A 2D coordination polymer with brick-wall network topology based on the [Cu(NCS)(2)(pn)] monomer. Inorg Chem Commun. 2007;10:815–20.

24. Powder diffraction file of the joint committee on powder diffraction standards. Sets 1-32. The International Center of Diffraction Data: Swarthmore, PA 19081, USA; 1982.

25. Mosmann T. Rapid colorimetric assay for cellular growth and survival—application to proliferation and cyto-toxicity assays. J Immunol Methods. 1983;65:55–63.

26. Netto AVG, Frem RCG, Mauro AE. Low-weight coordination polymers derived from the self-assembly reactions of Pd(II) pyrazolyl compounds and azide ion. Polyhedron. 2005;24: 1086–92.

27. Netto AVG, Frem RCG, Mauro AE, Crespi MS, Zorel HE Jr. Synthesis, spectral, and thermal studies on pyrazolate-bridged palladium(II) coordination polymers. J Therm Anal Calorim. 2007;87:789–92.

28. Netto AVG, Frem RCG, Mauro AE, Santos RHA, Zoia JR. Crystallographic and spectroscopic studies on palladium(II) complexes containing pyrazole and thiocyanate ligands. Transit Met Chem. 2002;27:279–83.

29. Netto AVG, Mauro AE, Frem RCG, Santana AM, Santos RHA, Zoia JR. Synthesis and structural characterization of dichlorobis(1-phenyl-3-methylpyrazole)palladium(II) and diazidobis(1-phenyl-3-methylpyrazole)palladium(II). J Coord Chem. 2001;54: 129–41.

30. Kargol JA, Crecely RW, Burmeister JL. ^{13}C nuclear magnetic resonance spectra of coordinated thiocyanate. Inorg Chim Acta. 1977;25:L109–10.

31. Netto AVG, Santana AM, Mauro AE, Frem RCG, de Almeida ET, Crespi MS, Zorel HE Jr. Thermal decomposition of palladium(II) pyrazolyl complexes. Part II. J Therm Anal Calorim. 2005;79:339–42.

32. Barra CV, Rocha FV, Netto AVG, Shimura B, Frem RCG, Mauro AE, Carlos IZ, Ananias SR, Quilles MB. New palladium(II) complexes with pyrazole ligands: Synthesis, spectral and thermal studies and antitumor evaluation, part I. J Therm Anal Calorim. 2010 (in press).

33. Netto AVG, Frem RCG, Mauro AE, de Almeida ET, Santana AM, de Souza J Jr. Santos RHA. Self-assembly of Pd(II) pyrazolyl complexes to 1-D hydrogen-bonded coordination polymers. Inorg Chim Acta. 2003;350:252–8.